Ultrafast Photochemistry of a Molybdenum Carbonyl-Nitrosyl Complex with a Triazacyclononane Coligand

Niklas Gessner,[a,b] Anna K. Bäck,[c] Johannes Knorr,[b] Christoph Nagel,[d] Philipp Marquetand,[c] Ulrich Schatzschneider,[d] Leticia González,[c] Patrick Nuernberger[a,b*]

SUPPORTING INFORMATION

[a.] *Institut für Physikalische und Theoretische Chemie, Universität Regensburg, Universitätsstraße 31, D-93053 Regensburg, Germany. E-Mail: patrick.nuernberger@ur.de; Tel: +49-941-943-4487*
[b.] *Former Address: Physikalische Chemie II, Ruhr-Universität Bochum, Universitätsstraße 150, D-44801 Bochum, Germany.*
[c.] *University of Vienna, Faculty of Chemistry, Institute of Theoretical Chemistry, Währinger Str. 17, A-1090 Wien, Austria.*
[d.] *Institut für Anorganische Chemie, Julius-Maximilians-Universität Würzburg, Am Hubland, D-97074 Würzburg, Germany.*

Vibrational signature of potential photoproducts

Gaussian 09 or ORCA; B3LYP-D3(BJ)/def2-SVP level of theory; acetonitrile as implicit solvent

Table S1. Unscaled vibrational band positions of the title complex as well as potential photoproducts. Corresponding structures are depicted in Figure S1 and the spectra are shown in Figure S2 to S4.

Species	$\tilde{\nu}$ (cm^{-1})	I (a.u.)	Mode	$\tilde{\nu}$ (cm^{-1})	I (a.u.)	Mode	$\tilde{\nu}$ (cm^{-1})	I (a.u.)	Mode
$[Mo(CO)_2(NO)(iPr_3tacn)]^+$	1772	2181	$\nu_{as}(MoNO)$	1998	2029	$\nu_{as}(Mo(CO)_2)$	2095	1192	$\nu_s(Mo(CO)_2)$
Ligand dissociation									
$[Mo(CO)(NO)(iPr_3tacn)]^{+\,\dagger}$	1724	1939	$\nu(NO)$ $\nu_{as}(N_{NO}MoC_{CO})$ $\omega(CH_3)$	1972	1704	ν_{as}(MoCO) $\nu_s(N_{NO}MoC_{CO})$	---	---	---
$[Mo(CO)_2(iPr_3tacn)]^{+\,*}$	1843	2527	$\nu_{as}(Mo(CO)_2)$	1983	1662	$\nu_s(Mo(CO)_2)$	---	---	---
$[Mo(CO)(iPr_3tacn)]^{+\,*}$	1819	2377	ν(CO)	2292	362	$\nu_{as}(MoNC_{ACN})$	---	---	---
NO isomerization									
bend *	1596	1946	$\nu_{as}(MoNO)$	1824	2398	$\nu_{as}(Mo(CO)_2)$	2952	1571	$\nu_s(Mo(CO)_2)$
1x CO-diss bend *	1505	1624	$\nu_{as}(MoNO)$	1789	2274	ν_{as}(MoCO)	2302	466	$\nu_s(MoACN)$
2x CO-diss bend *	1581	1838	$\tau(MoNO)$	1862	278	$\nu_s(MoACN)$	2260	971	$\nu_s(MoACN)$
	2946	203	$\nu_s(ACN\ CH_3)$	---	---	---	---	---	---
half flip *	1326	331	$\tau(MoNO)$	1843	2030	$\nu_{as}(Mo(CO)_2)$	1973	1841	$\nu_s(Mo(CO)_2)$
1x CO-diss half flip *	1241	347	$\tau(MoNO)$	1781	2150	$\nu_{as}(MoCO)$	2325	296	$\nu_{as}(MoACN)$
	929	383	ν(TACN)	1192	367	ν(NO)	1787	1910	$\nu_s(ACN)$
2x CO-diss half flip *	2292	661	$\nu_s(ACN)$	2960	267	$\nu_s(ACN\ CH_3)$	---	---	---
full flip †	1757	2307	$\nu_{as}(MoNO)$	1962	297	$\nu_{as}(Mo(CO)_2)$	2059	1277	$\nu_s(Mo(CO)_2)$ $\nu(MoO_{NO})$
1x CO-diss full flip *	1772	2146	$\nu_{as}(MoCO)$	2265	698	$\nu_s(MoACN)$			
Water coordination									
$[Mo(CO)(NO)(H_2O)(iPr_3tacn)]^{+\,*}$	1441	239	$\omega(tacn)$	1477	553	$\nu(NO)$ $\omega(tacn)$	1769	1884	$\nu_{as}(MoCO)$
	3802	327	$\nu_{as}(H_2O)$	---	---	---	---	---	---
$[Mo(NO)(H_2O)(iPr_3tacn)]^{+\,*}$	1548	1611	$\nu_{as}(MoNO)$	1822	367	$\nu_{as}(MoCN_{ACN})$	2940	215	$\nu_s(_{ACN}CH_3)$
	3784	357	$\nu_{as}(H_2O)$	---	---	---	---	---	---
$[Mo\ (NO)(H_2O)_2(iPr_3tacn)]^{+\,*}$	1480	201	$\omega(tacn)$	1521	306	$\tau(H_2O)$	1568	997	$\nu_{as}(MoNO)$
	2633	7164	$\nu_{as}(H_2O)$	2706	2433	$\nu_{as}(H_2O)$			

*Multiplicity assigned as singlet except: * doublet; Charge 0 except †: +1; ACN: acetonitrile; tacn: 1,4,7-tris(isopropyl)-1,4,7-triazacyclononane*

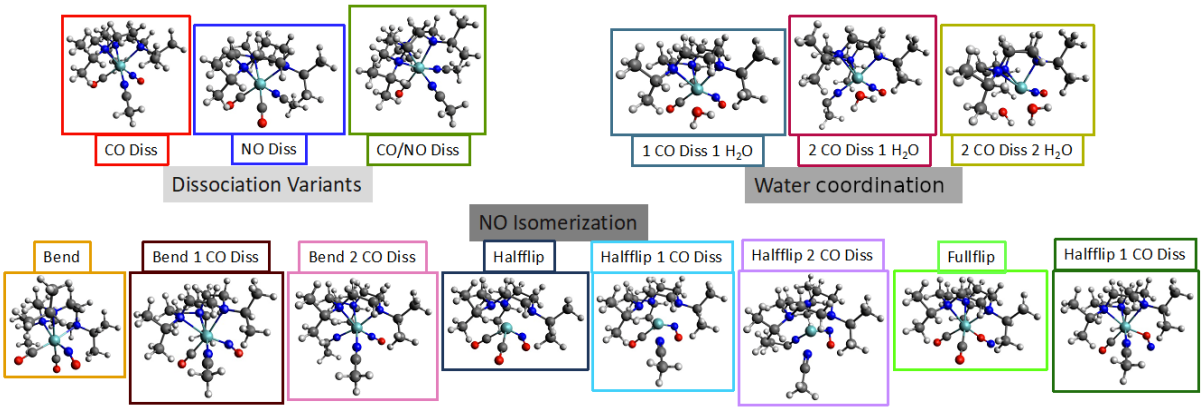

Figure S1. Three-dimensional structures of all considered potential photoproducts. The empty coordination site initially generated is assumed to be quickly occupied either by an acetonitrile solvent molecule or a water molecule from the environment present in small amounts during continuous UV light illumination of $[Mo(CO)_2(NO)(iPr_3tacn)]^+$ in acetonitrile (B3LYP-D3(BJ)/def2-SVP; implicit solvent acetonitrile).

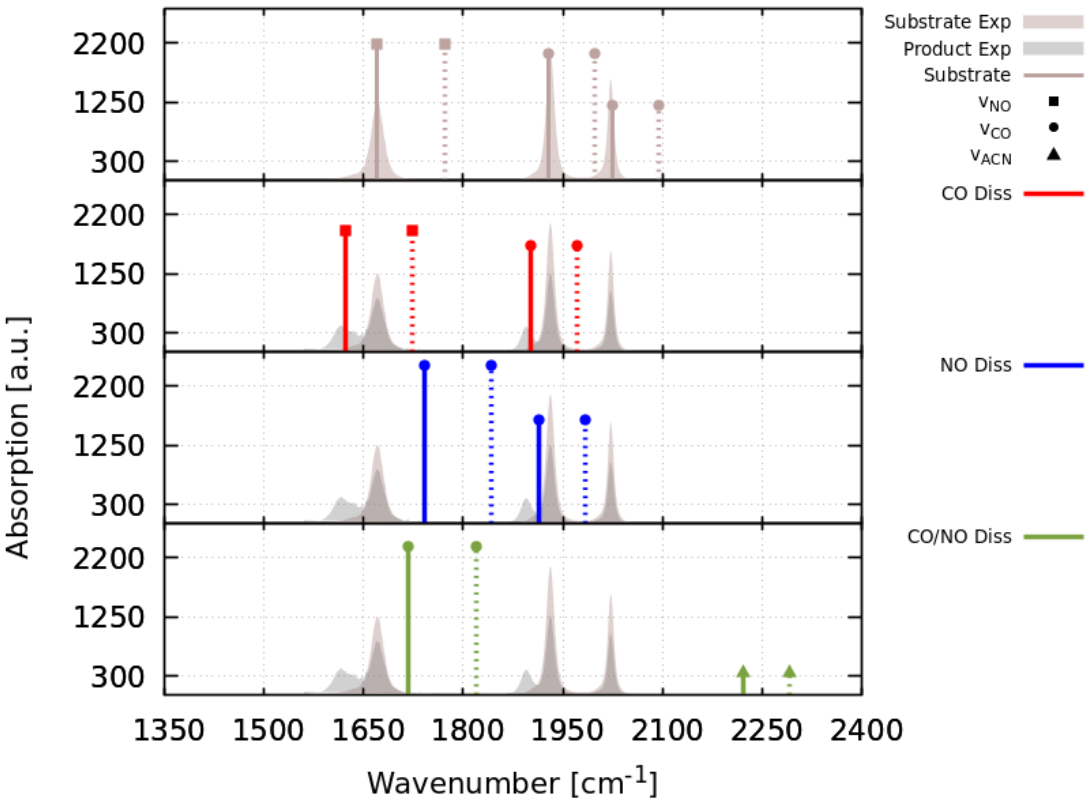

Figure S2. Calculated IR spectra of potential CO and/or NO loss photoproducts compared to the experimental spectrum. The simulated spectra without scaling are given as dashed lines while those with a red shift correction (101 cm^{-1} at ≤ 1905 cm^{-1} and 70 cm^{-1} at > 1905 cm^{-1}) are shown in continuous lines. The color coding corresponds to Figure S1 (DFT B3LYP-D3(BJ)/def2-SVP; acetonitrile as the implicit solvent).

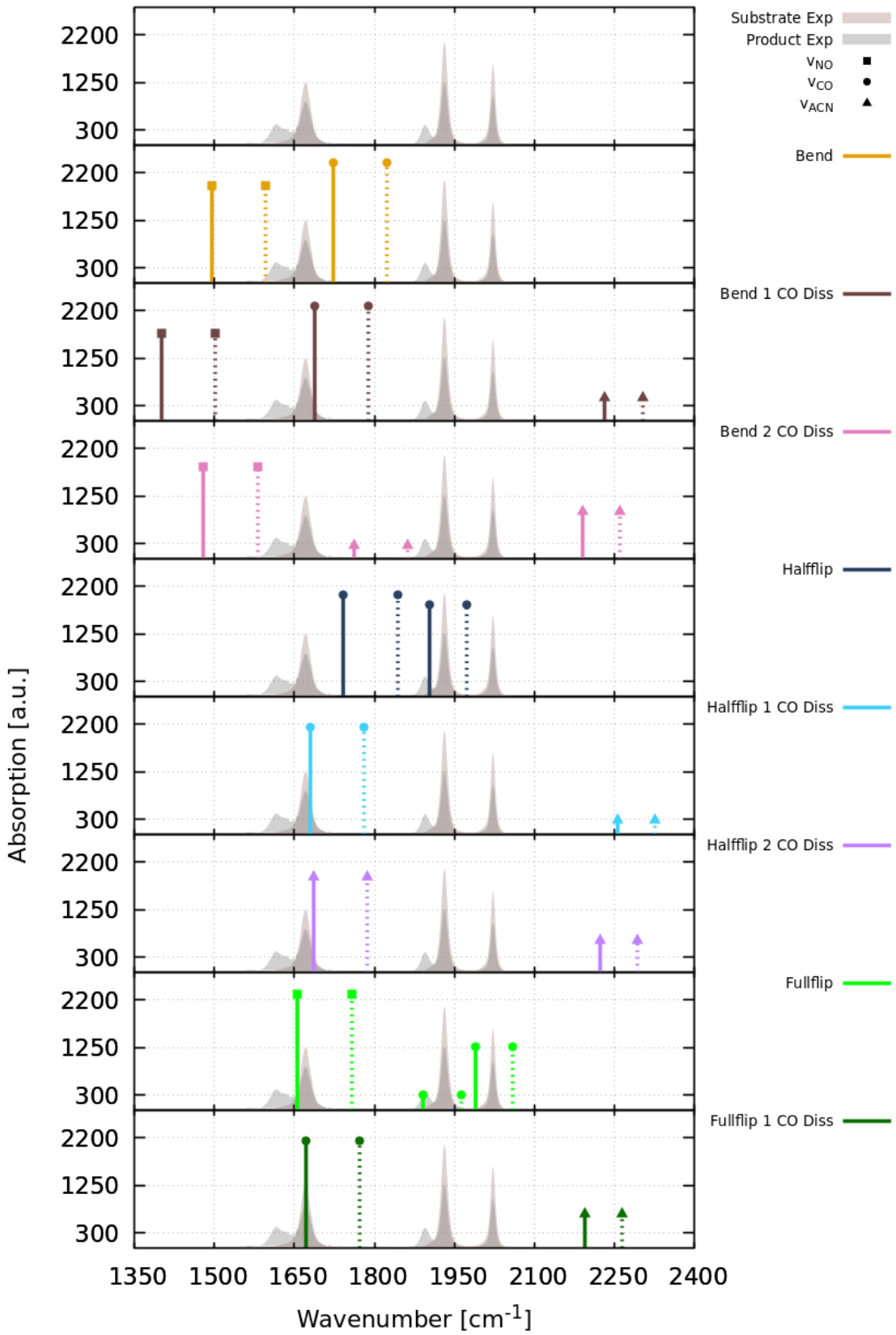

Figure S3. Calculated IR spectra of potential CO and/or NO loss photoproducts resulting from photolysis. Simulated spectra without scaling are given as dashed lines while those with a red shift correction (101 cm^{-1} at ≤ 1905 cm^{-1} and 70 cm^{-1} at > 1905 cm^{-1}) in continuous lines. The color coding corresponds to Figure S1 (DFT B3LYP-D3(BJ)/def2-SVP; acetonitrile as the implicit solvent).

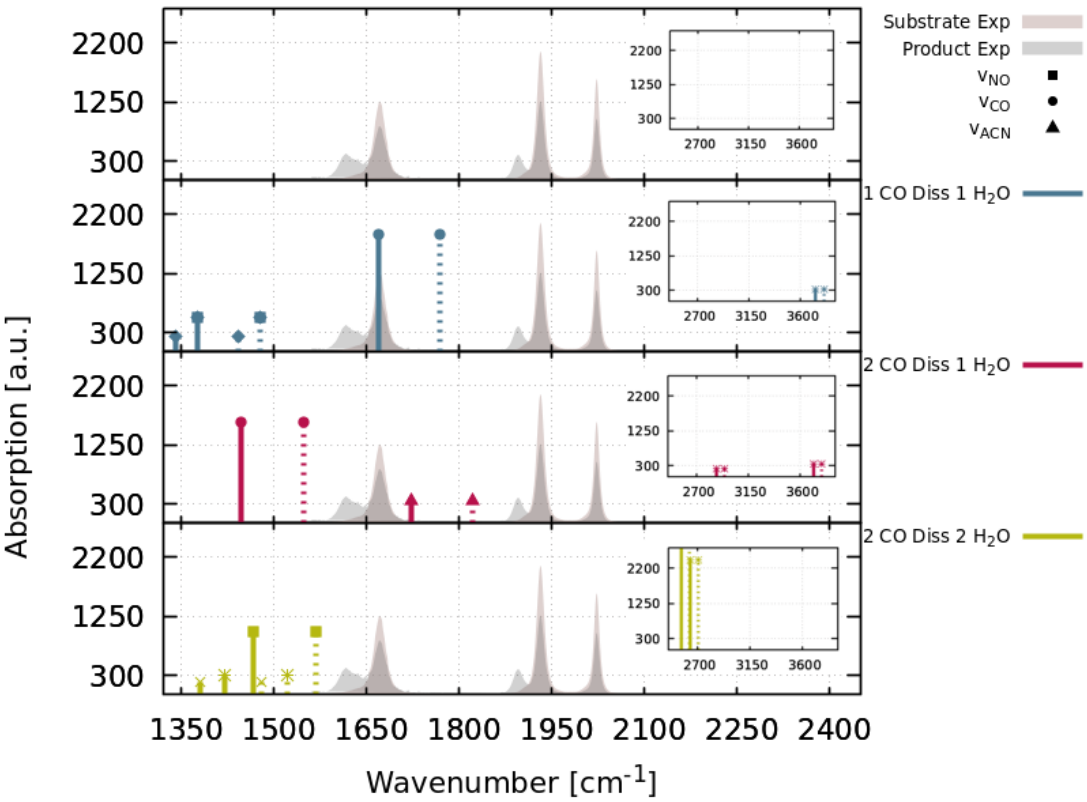

Figure S4. Calculated IR spectra of potential CO and/or NO "flip" photoproducts resulting from photolysis. Simulated spectra without scaling are given as dashed lines while those with a red shift correction (101 cm^{-1} at ≤ 1905 cm^{-1} and 70 cm^{-1} at > 1905 cm^{-1}) in continuous lines. The color coding corresponds to Figure S2 (DFT B3LYP-D3(BJ)/def2-SVP; acetonitrile as the implicit solvent)..

Voigt Profile Fit of FTIR Spectra

To determine the actual peak area and, thus, the absorption strength of each vibration, Voigt profiles $V(\tilde{\nu})$ were used to describe the line shape of all FTIR signals of intact complex **1** as well as the photoproduct observed. For the fit of the spectrum at t = 0, four functions were used in the model:

$$f(\tilde{\nu}) = \sum_{i=1}^{4} V_i(\tilde{\nu}) \ . \qquad \text{(eq. S1)}$$

Three Voigt profiles were used for the three main signals of CO and NO and one additional to describe the lower wavenumber edge of the NO peak. The resulting fit is shown as a purple solid line in Figure S5 for the NO region and in Figure S6 for the CO region, while data points are represented as dots. For each individual function that was normalized to its area, a parameter for the central wavenumber, the width of the Gaussian distribution, the width of the Lorentz distribution, and a peak area factor were optimized. The latter was used as the integral of each individual peak.

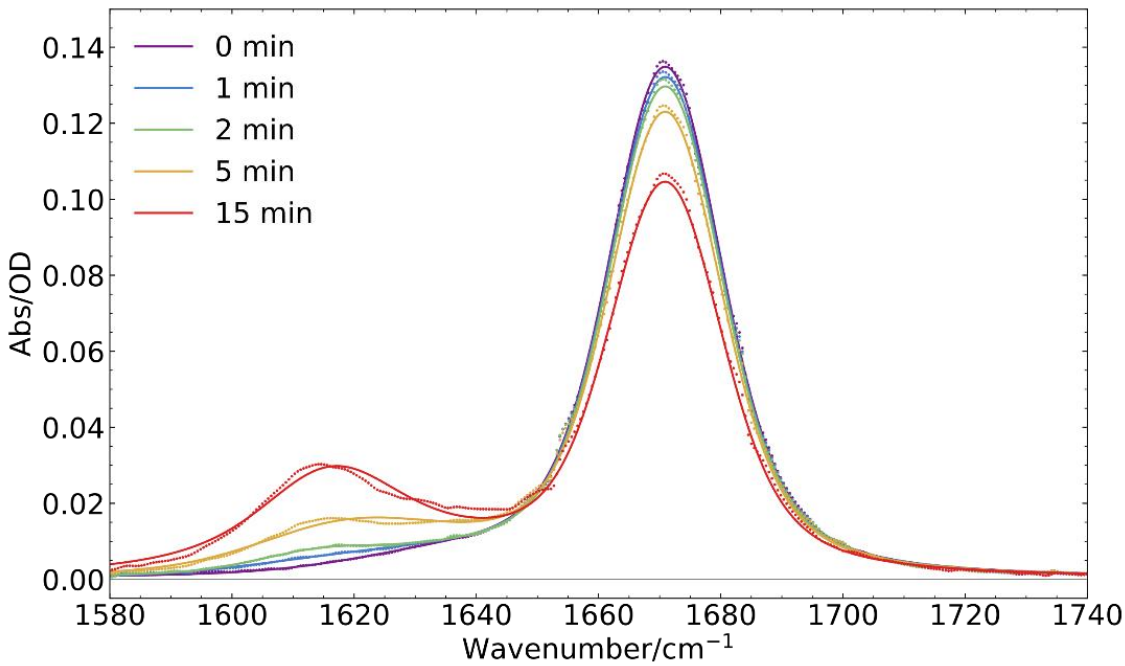

Figure S5. FTIR spectra of the NO region of the title complex recorded after different exposure times. The measured data points are shown as dots while the solid lines are the fit function.

For later spectra, all parameters of $f(\tilde{\nu})$ were kept fixed and a new model applied:

$$g(\tilde{\nu}) = S \cdot f(\tilde{\nu}) + \sum_{i=1}^{2} V_i(\tilde{\nu}) \qquad \text{(eq. S2)}$$

This uses a function f scaled by a parameter S and two additional Voigt profiles, one for each product peak. It is assumed that the concentration of **1** decreased in the course of the photolysis and thus, also the intensity of all of its peaks. The integral of these peaks is consequently calculated by multiplication of the corresponding integral at $t = 0$ and S. For the integral of the product peaks, the peak area parameter was used.

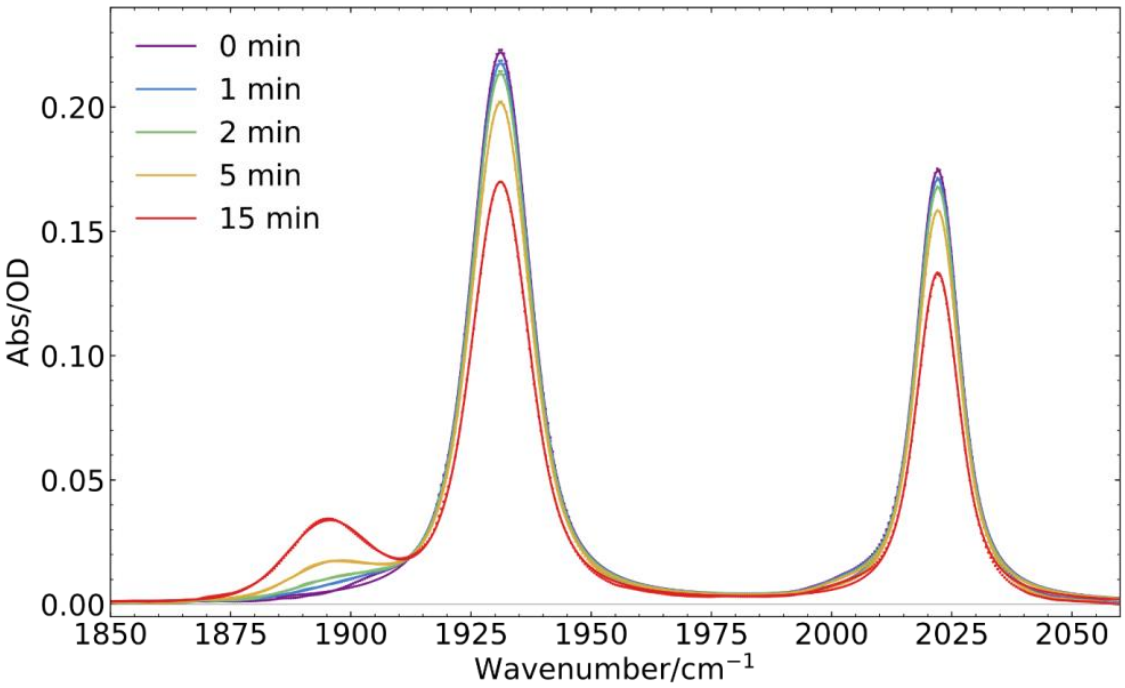

Figure S6. FTIR spectra of the CO region of the title complex **1** at different exposure times. The measured data points are shown as dots while the solid line is the fitted function.

Geometric features of optimized geometry

Gaussian09; B3LYP-D3(BJ)/def2-SVP level of theory; implicit solvent acetonitrile

Table S2. Comparison of experimental X-ray structural data and calculated bond lengths (Å) and angles (°) for*[Mo(CO)$_2$(NO)(iPr$_3$tacn)]$^+$* at the lowest ground state minimum.

Bond lengths	X-ray (Å)	DFT (Å)
Mo(1)-C(2)	1.954(2)	2.01
Mo(1)-C(4)	1.963(2)	2.00
Mo(1)-N_{NO}(6)	1.8808(19)	1.79
Mo(1)-N_{tacn}(14)	2.3023(15)	2.34
Mo(1)-N_{tacn}(15)	2.3102(16)	2.39
Mo(1)-N_{tacn}(16)	2.3010(16)	2.32
C(2)-O(3)	1.160(2)	1.15
C(4)-O(5)	1.161(2)	1.15
N(6)-O(7)	1.188(2)	1.18
Bond angles angle	**X-ray (°)**	**DFT (°)**
Mo(1)-C(2)-O(3)	177.27(17)	176
Mo(1)-C(4)-O(5)	174.88(17)	178
Mo(1)-N(6)-O(7)	175.27(16)	178
Mo(1)-N_{tacn}(14)-C_{iPr}(17)	114.80(11)	116
Mo(1)-N_{tacn}(15)-C_{iPr}(37)	116.16(11)	116
Mo(1)-N_{tacn}(16)-C_{iPr}(27)	116.55(12)	116

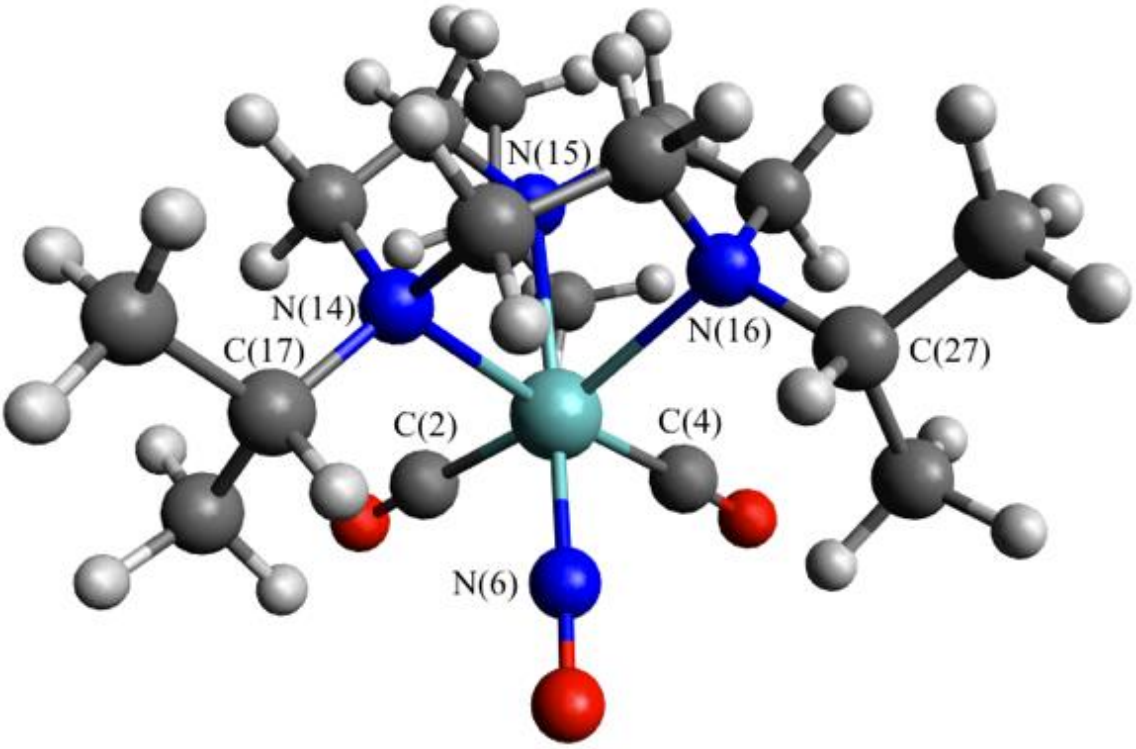

Figure S7. Optimized geometry of [Mo(CO)$_2$(NO)(iPr$_3$tacn)]$^+$ at the lowest ground state minimum.

XYZ coordinates of the optimized geometry of $[Mo(CO)_2(NO)(iPr_3tacn)]^+$

```
58

Mo   -0.885875    0.530756    0.371596
C   -2.721736    0.219617    1.118365
O   -3.740128    0.028200    1.622596
C   -0.948027    2.335881    1.222217
O   -1.027865    3.367872    1.730851
N   -0.191048   -0.155152    1.875990
O    0.295950   -0.586752    2.857962
C    0.957674    1.869472   -1.619028
C   -0.292254    1.752563   -2.475659
C   -2.307892    0.305182   -2.450076
C   -2.205059   -1.092517   -1.816416
C    0.236166   -1.236747   -1.962690
C    1.435203   -0.560833   -1.326234
N   -0.949895   -1.326565   -1.053902
N   -1.571083    1.410152   -1.740660
N    1.173204    0.753409   -0.663440
C   -0.944879   -2.691745   -0.378661
C   -1.222040   -3.840302   -1.357203
C   -1.894015   -2.812208    0.810661
H    0.084039   -2.793090   -0.001402
H   -0.648590   -3.770188   -2.292351
H   -0.942595   -4.789066   -0.875190
H   -2.291006   -3.904204   -1.612817
H   -1.621195   -2.156512    1.644608
H   -2.940299   -2.619101    0.531121
H   -1.847950   -3.847057    1.182316
C    2.365785    1.041378    0.246221
C    2.154628    2.187442    1.231240
C    3.666399    1.263115   -0.535443
H    2.474607    0.118035    0.833125
H    1.403389    1.952927    1.993640
H    3.104272    2.363425    1.758708
H    1.882129    3.132255    0.738171
H    3.858634    0.485618   -1.287498
H    3.682484    2.244085   -1.035365
H    4.507810    1.244260    0.173192
C   -2.428318    2.672663   -1.691755
C   -3.624264    2.565738   -0.750671
C   -2.913603    3.111807   -3.079615
H   -1.747714    3.444620   -1.301946
H   -3.336228    2.521869    0.305437
H   -4.250963    3.461363   -0.875522
H   -4.256917    1.694451   -0.979814
H   -2.119710    3.117522   -3.839374
H   -3.731052    2.471483   -3.444522
H   -3.306427    4.137101   -3.007936
H    2.211455   -0.458980   -2.100840
H    1.840610   -1.219767   -0.545904
H    0.562701   -2.239773   -2.267299
H   -0.060160   -0.744150   -2.889614
H   -2.312422   -1.828966   -2.628164
H   -3.041447   -1.248715   -1.125277
H   -1.973667    0.277112   -3.495187
H   -3.374923    0.549542   -2.480258
H   -0.405974    2.720822   -2.977791
H   -0.138954    1.028175   -3.278358
H    1.810283    1.965419   -2.311194
H    0.911355    2.792961   -1.028343
```

Full charge transfer characterization

ORCA and TheoDORE; TD-B3LYP-D3(BJ)/def2-SVP level of theory; implicit solvent acetonitrile

Table S3. Energy differences (Δ*E* in eV) to the ground state, oscillator strengths (f in a.u.), and the two most important state characters of the 16 lowest excited singlet and 22 lowest triplet states of $[Mo(CO)_2(NO)(iPr_3tacn)]^+$ at geometry of the ground-state minimum.

state	ΔE(eV)	*f* (a.u.)	character		state	ΔE(eV)	*f* (a.u.)	character	
			main	secondary				main	secondary
T_1	2.57	0.000	$ML_{NO}CT$	$L_{NO}C$	T_{14}	4.60	0.000	$ML_{CO}CT$	$L_{NO}L_{CO}CT$
T_2	2.66	0.000	$ML_{NO}CT$	$ML_{CO}CT$	T_{15}	4.61	0.000	$ML_{CO}CT$	MC
T_3	2.81	0.000	$ML_{NO}CT$	$ML_{CO}CT$	T_{16}	4.61	0.000	$ML_{CO}CT$	MC
T_4	2.82	0.000	$ML_{NO}CT$	$L_{NO}C$	T_{17}	4.72	0.000	$ML_{CO}CT$	$L_{NO}L_{CO}CT$
S_1	2.88	0.000	$ML_{NO}CT$	$ML_{CO}CT$	T_{18}	4.73	0.000	$L_{tacn}L_{NO}CT$	$L_{tacn}L_{CO}CT$
T_5	2.95	0.000	$ML_{NO}CT$	$L_{NO}C$	S_7	4.76	0.014	$ML_{CO}CT$	MC
S_2	3.06	0.001	$ML_{NO}CT$	$ML_{CO}CT$	T_{19}	4.77	0.000	$L_{tacn}L_{NO}CT$	$L_{tacn}L_{CO}CT$
S_3	3.29	0.001	$ML_{NO}CT$	$L_{NO}C$	S_8	4.77	0.016	$ML_{CO}CT$	$L_{NO}L_{CO}CT$
T_6	3.36	0.000	$ML_{NO}CT$	$L_{NO}C$	S_9	4.87	0.005	$ML_{CO}CT$	$L_{NO}L_{CO}CT$
S_4	3.56	0.001	$ML_{NO}CT$	$L_{NO}C$	S_{10}	4.94	0.001	$L_{tacn}L_{NO}CT$	$L_{tacn}L_{CO}CT$
S_5	3.67	0.006	$ML_{NO}CT$	$L_{NO}C$	S_{11}	4.94	0.001	$L_{tacn}L_{NO}CT$	$L_{tacn}L_{CO}CT$
T_7	3.75	0.000	$ML_{CO}CT$	$L_{CO}C$	S_{12}	4.99	0.001	$ML_{CO}CT$	MC
T_8	4.09	0.000	$ML_{CO}CT$	MC	T_{20}	5.02	0.000	$L_{tacn}L_{NO}CT$	$L_{tacn}L_{CO}CT$
T_9	4.16	0.000	$ML_{CO}CT$	MC	S_{13}	5.02	0.006	$ML_{CO}CT$	$L_{NO}L_{CO}CT$
S_6	4.46	0.001	MC	$ML_{CO}CT$	S_{14}	5.02	0.000	$L_{tacn}L_{NO}CT$	$L_{tacn}L_{CO}CT$
T_{10}	4.52	0.000	$ML_{CO}CT$	$L_{NO}L_{CO}CT$	S_{15}	5.12	0.001	$L_{tacn}L_{NO}CT$	$L_{tacn}L_{CO}CT$
T_{11}	4.56	0.000	$L_{tacn}L_{NO}CT$	$L_{tacn}L_{CO}CT$	S_{16}	5.16	0.001	$L_{tacn}L_{NO}CT$	$L_{tacn}L_{CO}CT$
T_{12}	4.56	0.000	$L_{tacn}L_{NO}CT$	$L_{tacn}L_{CO}CT$	T_{21}	5.17	0.000	MC	$ML_{CO}CT$
T_{13}	4.57	0.000	$L_{tacn}L_{NO}CT$	$L_{tacn}L_{CO}CT$	T_{22}	5.21	0.000	$ML_{CO}CT$	$L_{NO}L_{CO}CT$

Potential energy scan

MOLCAS; SA-CASSCF(8,10)/ANO-RCC-MB; gas phase; geometry optimization B3LYP-D3(BJ)/def2-TZVPP; gas phase

Table S4. Raw data of potential energy scan plotted in Figure 11 given as relative energies to the ground state of the equilibrium geometry (SA-CASSCF(8,10)/ANO-RCC-MB; gas phase).

distance (Å)	ΔE(eV)							
	S_0	S_1	S_2	S_3	S_4	S_5	S_6	S_7
CO dissociation								
2.0	0.00	2.78	3.09	3.92	4.26	4.32	5.03	5.28
2.1	0.00	2.70	3.08	3.98	4.30	4.44	4.75	5.09
2.3	0.14	2.69	3.35	4.13	4.46	4.71	4.75	5.09
2.5	0.37	2.85	3.74	4.14	4.34	4.61	4.82	5.06
2.8	0.63	3.06	3.51	4.32	4.40	4.54	4.92	5.01
3.1	0.80	3.22	3.32	4.21	4.42	4.64	4.85	5.17
3.5	0.94	3.15	3.37	4.05	4.36	4.71	4.93	5.31
3.9	1.01	3.07	3.45	3.98	4.30	4.76	4.99	5.36
4.5	1.07	3.02	3.51	3.94	4.26	4.80	5.05	5.39
5.2	1.09	3.01	3.53	3.94	4.24	4.82	5.08	5.39
7.1	1.12	3.01	3.56	3.95	4.25	4.84	5.10	5.39
10.0	1.12	3.01	3.56	3.95	4.25	4.85	5.11	5.40
NO dissociation								
1.8	0.00	2.85	3.09	3.94	4.28	4.33	5.00	5.27
1.9	0.17	2.50	2.65	3.28	3.60	3.64	4.87	5.13
2.1	0.68	2.64	2.77	3.05	3.29	3.38	5.20	5.37
2.4	1.90	2.81	3.03	3.19	3.40	3.48	5.69	5.90
2.7	2.65	2.92	3.19	3.32	3.71	3.73	6.09	6.12
3.0	2.94	3.01	3.35	3.41	3.84	3.85	6.27	6.28
3.3	3.08	3.11	3.42	3.45	3.87	3.87	6.38	6.39
3.9	3.28	3.28	3.50	3.50	3.89	3.89	6.30	6.31
4.5	3.33	3.33	3.54	3.54	3.94	3.94	6.20	6.20
5.2	3.39	3.39	3.80	3.81	4.05	4.05	4.97	4.97
7.1	3.39	3.39	3.80	3.80	4.05	4.05	4.96	4.96
10.0	3.38	3.38	3.80	3.80	4.04	4.04	4.95	4.95